arXiv:1408.4741v1 [astro-ph.HE] 20 Aug 2014

Discovery of X-ray pulsations from *next Geminga* — PSR J1836+5925

L. C. C. Lin[1], C. Y. Hui[2], K. T. Li[3], J. Takata[4], C. P. Hu[5], A. K. H. Kong[1], D. C. C. Yen[6] and Y. Chou[5]

cyhui@cnu.ac.kr

ABSTRACT

We report the X-ray pulsation of ~ 173.3 ms for the "*next Geminga*", PSR J1836+5925, with recent *XMM-Newton* investigations. The X-ray periodicity is consistent wtih the γ-ray ephemeris at the same epoch. The X-ray folded light curve has a sinusoidal structure which is different from the double-peaked γ-ray pulse profile. We have also analysed the X-ray phase-averaged spectra which shows the X-ray emission from PSR J1836+5925 is thermal dominant. This suggests the X-ray pulsation mainly originates from the modulated hot spot on the stellar surface.

Subject headings: Gamma rays: general — pulsars: general — pulsars: individual (PSR J1836+5925) — radiation mechanisms: non-thermal — radiation mechanisms: thermal — X-rays: general

1. Introduction

The launch of *Fermi* Gamma-ray Space Telescope in 2008 provides the opportunity to examine γ-rays emitted from compact objects, and 117 γ-ray pulsars has been detected with the first three years archival data (Abdo et al. 2013). Among all the pulsars detected by *Fermi*, 36 were directly found by the blind search in the γ-ray band and 34 of them were identified as radio-quiet with the threshold of 30 μJy in radio flux density at 1400 MHz. The population of radio-quiet γ-ray pulsars is expanding due to the continuous accumulation of *Fermi* data and the improvement of the searching schemes (e.g., weighting H test-statistic; Kerr 2011). This has imposed constraints on the pulsar emission geometry which suggests the radio emission and the γ-rays are not produced in the same region of the pulsar magnetopshere. While the radio emission is originated from the cones emerged near the stellar surface, the pulsed γ-rays are generally accepted to arise from the outer magnetosphere (cf. Cheng & Zhang 1998; Takata et al. 2006, 2008). The radio-quiet pulsars can be resulted from their different orientation of their radio beam and the observer's line-of-sight. Therefore, determining the emission geometry (e.g. magnetic inclination, viewing angle) is important for a better understanding of their properties. However, the lack of knowledge in the phase relationship between the γ-ray light curves and that in radio leads to an ambiguity in determining which peak in the γ-ray light curves is leading (see Trepl et al. 2010 for a more detailed discussion). Therefore, pulsation searches in the other wavelengths, in particular in X-ray, are needed.

Only four of them have the X-ray pulsation detected so far (Halpern & Holt 1992; Lin et al. 2010; Lin et al. 2013; Marelli et al. 2014). For those pulsars whose periodicities can only be detected in both X-ray and γ-ray bands are usually classified as Geminga-like pulsars with Geminga

[1]Institute of Astronomy, National Tsing-Hua University, Hsinchu 30013, Taiwan

[2]Department of Astronomy and Space Science, Chungnam National University, Daejeon, South Korea

[3]Department of Biological Science and Technology, China Medical University, Taichung 40402, Taiwan

[4]Department of Physics, University of Hong Kong, Pokfulam Road, Hong Kong, PRC

[5]Graduate Institute of Astronomy, National Central University, Jhongli 32001, Taiwan

[6]Department of Mathematics, Fu Jen Catholic University, New Taipei City 24205, Taiwan

(i.e. PSR B0633+17) as the prototypical example of this class (Halpern & Holt 1992; Bertsch et al. 1992). X-ray pulsations of three other known Geminga-like pulsars, PSR J0007+7302 (Lin et al. 2010; Caraveo et al. 2010), PSR J2021+4026 (Lin et al. 2013) and PSR J1813-1246 (Marelli et al. 2014) were subsequently discovered. Except for PSR J1813-1246 which has a very hard non-thermal dominant X-ray spectrum, the phase-averaged spectrum of other three Geminga-like pulsars have multicomponent which consists of a non-thermal contribution and at least one thermal component (Caraveo et al. 2004; Lin et al. 2010, 2013; Caraveo et al. 2010). The pulse profiles in X-ray and γ-ray are dissimilar with an obvious offset (Caraveo et al. 2010; Lin et al. 2010, 2013). This suggests the pulsed emission in these two regimes are originated from different regions. While the aforementioned three pulsars have similar X-ray/gamma-ray properties, we note that the derived paramaters (e.g. characteristic age, magnetic field and spin-down power) of PSR J0007+7302 and PSR J2021+4026 are rather different from Geminga.

On the other hand, the X-ray counterpart of 3EG J1835+5928, RX J1836.2+5925, identified by Mirabal et al. (2000) and Mirabal & Halpern (2001) has been considered as the "next Geminga" for a long time because of the lack of radio detection (a flux density of the radio observation at a frequency of 1.4 GHz $< 3\mu$Jy; Abdo et al. 2010), the similar spectral behavior and γ-ray luminosity to Geminga (Halpern et al. 2002). The γ-ray pulsation of this source was finally detected by Abdo et al. (2009), and it was classified as a middle-aged pulsar ($\sim$ 1800 kyr) that is similar to Geminga. The surface magnetic field ($\sim 5 \times 10^{11}$ G) and the spin-down power ($\sim 1.2 \times 10^{34}$ erg s^{-1}) of PSR J1836+5925 is about 1/3 to those of Geminga although its spin efficiency to convert γ-rays is about one order of magnitude higher (Abdo et al. 2010). However, the lack of the pulsation detected in other wavelengths does not allow us to compare the emission properties at different energies. Therefore, periodicity searches at other energies, particularly in X-ray band, are require to constrain its high energy emission properties and enable us to compare its nature with other Geminga-like pulsars. The X-ray pulsation have been long sought for this target (Halpern et al. 2007; Abdo et al. 2010). However, no positive detection has been reported yet.

Using the archival *XMM-Newton* data of PSR J1836+5925, we have performed a detailed temporal and spectral analysis observations. In this Letter, we report the results from this investigation. In particular, we report the discovery of the X-ray pulsations from PSR J1836+5925 for the first time.

2. Observations and data analysis

The latest *XMM-Newton* observations of PSR J1836+5925 were on 2013 February 14 and 16 (hereafter 0214 and 0216) have a total exposure of $\sim$ 44 and 39 ks (Obs. ID: 0693090101 and 0693090201; PI: Pavlov G.). During these observations, the satellite was pointed to RA=$18^{\rm h}36^{\rm m}13.75^{\rm s}$ Dec=$+59^{\circ}25^{'}30.3^{''}$ (J2000), which is the timing position of the γ-ray ephemeris determined by Abdo et al. (2010). In both observations, MOS1/2 CCDs were operated in full-window mode and PN CCD was operated in small-window mode with a temporal resolution of $\sim$5.7 ms which enables us to search for X-ray pulsations. We reprocessed all the raw data with the tasks *emchain* and *epchain* in XMM-Newton **S**cience **A**nalysis **S**oftware (XMMSAS version 13.5.0). For a rigorous analysis, we have excluded those events next to the edges of CCDs and bad pixels, which may have incorrect energies. The good events with "PATTERN" for MOS1/2 were selected in range of 0-12 to include single to quadruple pixel events, and those for the PN in the range 0-4 to include only single and double events. In our analysis, we only consider the events in the energy range of $0.2 - 12$ keV. We also noted that all investigations have been contaminated by the X-ray background flare. After removing all events which are potentially contaminated, the effective exposures were found to be 41.1 ks, 41.3 ks and 41.4 ks for MOS1, MOS2, PN observed on 0214 and 32.3 ks, 32.2 ks and 32.8 ks for MOS1, MOS2, PN observed on 0216, respectively. We determined the position of PSR J1836+5925 in each dataset with the XMMSAS task *edetect_chain*.

2.1. Timing analysis

For searching X-ray pulsations from PSR J1836+5925, we utilized the PN data obtained in both observations. Its nominal X-ray position in 0214

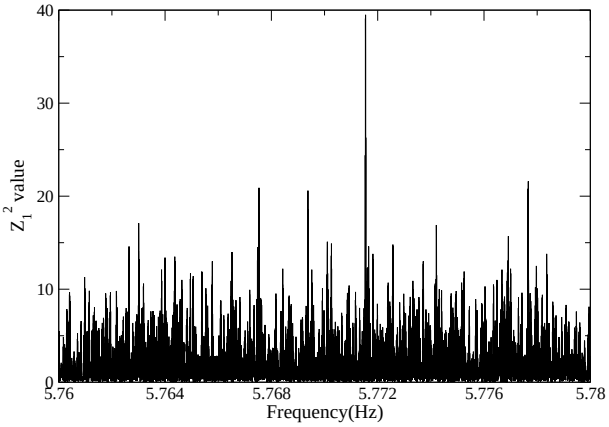

Fig. 1.— Detection of X-ray pulsation on PSR J1836+5925. The periodogram of Rayleigh-test in the frequency range of 5.76-5.78 Hz. The independent trial in the search corresponds to the Fourier resolution of this observation (i.e. $\sim 4.76 \times 10^{-6}$ Hz).

adn 0216 are R.A.=$18^h36^m13^s.68$, decl.=+59° 25′30″.72 (J2000) (with the uncertainty $\sim$ 0″.5) and R.A.=$18^h36^m13^s.92$, decl.=+59°25′29″.64 (with the uncertainty $\sim$ 0″.7). Within the statisical uncertainties, they are consistent to the position determined by *Chandra*/ACIS (Advanced CCD Imaging Camera), *Chandra*/HRC (High Resolution Camera) (Halpern et al. 2002, 2007) and the γ-ray timing position determined in Abdo et al. (2010). Since *Chandra*/HRC provides the most accurate positional determination, we adopted the position determined by this instrument, R.A.=$18^h36^m13^s.674$, decl.=+59°25′30″.15 (J2000) for the barycentric correction. Events within a circular region of a 20″ radius centered at this position which corresponds to an encircle energy function of $\sim$ 76% were extracted. We have 992 counts on 0214 and 806 counts on 0216 available for the timing analysis. We then corrected the photon arrival times to Barycentric Dynamical Time (TDB) with the aforementioned X-ray position and JPL Solar System ephemeris DE 405 using the XMMSAS task of *barycen*.

We noted that the $\gamma-$ray timing position of PSR J1836+5925 in the available ephemerides has a small offset from our adopted X-ray position. For consistency, we constructed a new local ephemeris of this pulsar to cover the epoch of these recent *XMM-Newton* investigations (i.e. $\sim$MJD 56338). We used the *Fermi* Science Tools v9r27p1 package to perform the data reduction. We obtained the *Fermi* LAT data in the energy range of 0.1-300 GeV within a circular region of interest (ROI) with a 0.8° radius from the decided X-ray position of PSR J1836+5925. We used Pass 7 data and selected events in the "Source" class (i.e. event class 2). Only a data span of $\sim$ 1 year, which brackets the epoch of two recent *XMM-Newton* observations, were considered to avoid accumulated effects due to the timing noise propagated from a long-term data. We also excluded the events with zenith angles larger than 100° to reduce the contamination by the Earth albedo γ-rays. For determining the pulse times of arrivals (TOAs), we built a template with the latest ephemeris reported by *Fermi* collaboration [1] by means of Gaussian kernal density estimation (KDE). We have obtained 25 TOAs by cross-correlating the template with the unbinned geocentered data. Each event was assigned to a phase according to the KDE model. With the position fixed at that determined by *Chandra*/HRC (Halpern et al. 2007), we fitted the TOAs with TEMPO2 (Hobbs et al. 2006; Edwards et al. 2006) to obtain a timing solution for PSR J1836+5925 that includes a spin frequency (f), a spin-down rate ($\dot{f}$) and a second derivative of frequency ($\ddot{f}$). The results are summarized in Table 1.

Table 1: Local ephemeris of PSR J1836+5925 derived from LAT data which brackets the latest *XMM-Newton* observations on MJD 56337.45 and MJD 56339.44. The numbers in parentheses denote errors in the last digit.

Pulsar name	PSR J1836+5925
Valid MJD range	56147.8—56522.2
Right ascension, α	18:36:13.674
Declination, δ	+59:25:30.15
Pulse frequency, f (s^{-1})	5.7715448470(3)
First derivative of pulse frequency, $\dot{f}$ (s^{-2})	$-5.002(3) \times 10^{-14}$
second derivative of pulse frequency, $\ddot{f}$ (s^{-3})	$-1(1) \times 10^{-23}$
Epoch of frequency determination (MJD)	56338
Solar system ephemeris model	DE405
Time system	TDB

Using the $\gamma-$ray ephemeris which is contem-

[1] https://confluence.slac.stanford.edu/display/GLAMCOG/LAT+Gamma-ray+Pulsar+Timing+Models

poraneous with recent X-ray observations, we can compare temporal properties in both regimes. We directly folded up the PN data with the spin parameters in Table 1. For the data in 0.2-12 keV, the random probability to yield the X-ray pulsation of 5.7715448470(3) Hz at epoch of MJD 56338 is $\sim 3.6 \times 10^{-7}$ (H test-statistic (TS) = 37.1) with a single harmonic (de Jager & Büsching 2010). We have also computed the periodogram of Rayleigh-test in the frequency range 5.76-5.78 Hz which is shown in Figure 1. It clearly shows an X-ray periodic signal at 5.771545(5) Hz with $Z_1^2 = H\ TS = 39.5$. The quoted error of the frequency corresponds to the Fourier resolution of this observation (Leahy 1987). This is consistent with the pulse frequency in γ-ray regime. To compare the pulse profiles between X-rays and γ-rays, we folded all the photons extracted from *XMM-Newton* observations and those obtained from *Fermi* observations within MJD 56150–56520 in accordance with the $\gamma-$ray ephemeris Table 1. We also divided the obtained X-ray events into three different energy bands, which are similar to the studies of three other Geminga-like pulsars (Caraveo et al. 2004, 2010; Lin et al. 2013). The phase-aligned folded light curves at different energy ranges are shown in Fig. 2. For the X-ray light curves, we have subtracted the background sampled from a nearby circular region with a radius of 20" centered at R.A.=$18^h36^m20^s.752$, decl.=$+59°26'07''.92$ (J2000). The X-ray pulsation can be firmly detected in the soft X-ray band (H TS=23.6 with a random probability of $\sim 7.9\times10^{-5}$) and marginally found in the medium X-ray band (H TS=11.6 with a random probability of $\sim 9.7 \times 10^{-3}$). Nevertheless, the significance is too low for claiming the detection in the hard band (H TS=4.0 with a random probability of 0.2), which can be ascribed to the small photon statistic.

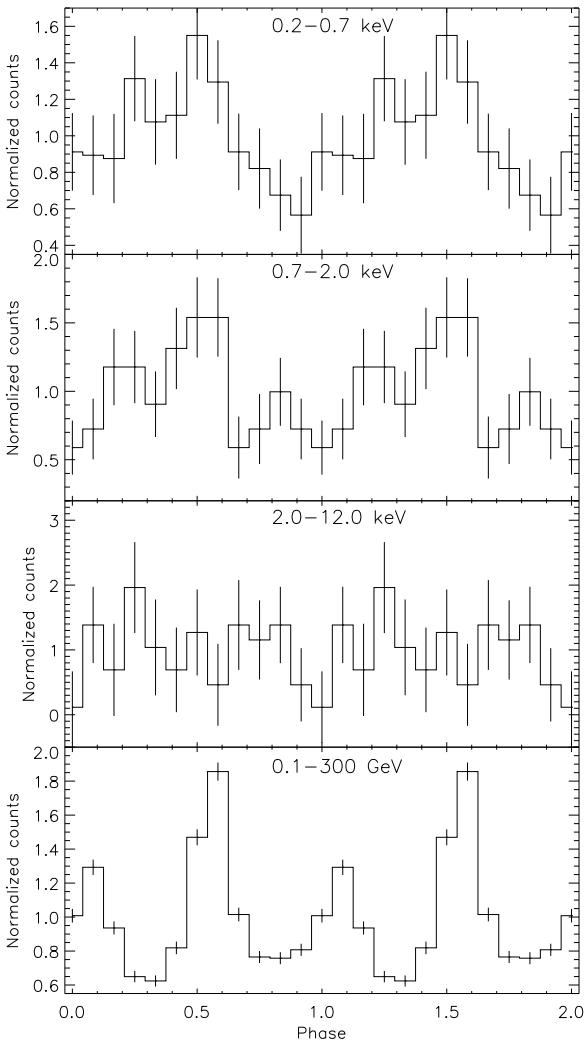

Fig. 2.— Folded light curves of PSR J1836+5925 in different energy ranges. Each panel shows the pulse profile of 12 bins in the energy band specified in the legend. The epoch/phase zero of all the profiles were determined at MJD 56338 shown in Table 1.

2.2. Spectral analysis

Because our adopted data have the total exposures of more than 80 ks, this enables us to place a tighter constraint on the X-ray spectral properties of PSR J1836+5925 than the previous investigations (Halpern et al. 2002; Abdo et al. 2010). We extracted the spectra of PSR J1836+5925 from a circle with a radius of $20''$ centered at its nominal position in each EPIC data. The background spectra were sampled from a nearby circular source-free region with a radius of $20''$ in individual dataset. We generated the response matrices and ancillary response files with the XMMSAS task *rmfgen* and *arfgen*. Since the X-ray emission from PSR J1836+5925 is relatively soft, we considered X-ray spectral fits in the energy range of 0.2–5 keV. We grouped each spectrum so as to have a minimum of 15 counts in each bin. We have exam-

ined each dataset individually and found that the inferred parameters are consistent within the tolerance of the uncertainties. In order to optimize the photon statistics, we fitted all the EPIC data obtained in these two observations simultaneously. The errors of the spectral parameters quoted in this Letter are in 1σ for 2 parameters of interest (i.e. $\Delta\chi^2 = 2.30$ above the minimum) for single component models and in 1σ for 4 parameters of interest (i.e. $\Delta\chi^2 = 4.72$ above the minimum) for multi-component models.

For the tested single component models (i.e. power-law and backbody), none of them can result in a statistically reasonable fit (with reduced $\chi^2 > 1.5$). It may indicate that the X-ray emission of PSR J1836+5925 comprises more than one spectral component. Therefore, we proceeded to fit the data with multicomponent spectral models. We have found that the spectrum can be described by an absorbed blackbody plus power-law model. We firstly attempted to perform the fitting with all parameters to be free, which yields a column absorption of $n_{\rm H} < 8.5 \times 10^{19}$ cm^{-2}, a photon index of $\Gamma = 1.8 \pm 0.3$, a power-law model normalization of $6.0^{+1.3}_{-1.2} \times 10^{-6}$ photons keV^{-1} cm^{-2} s^{-1} at 1 keV, a blackbody temperature of $kT = 62^{+11}_{-10}$ eV with a emission radius of $R = 1.32^{+2.37}_{-0.55}$ km at 800 pc. This results in a desirable goodness-of-fit ($\chi^2 = 90.46$ for 85 d.o.f.).

As the column absorption cannot be properly constrained, we also fitted the data with $n_{\rm H}$ fixed at total Galactic HI column density of 4×10^{20} cm^{-2} in the direction of PSR J1836+5925 (Kalberla et al. 2005). This yields the best-fit parameters of $\Gamma = 2.1 \pm 0.3$, a power-law model normalization of $(7.1 \pm 1.4) \times 10^{-6}$ photons keV^{-1} cm^{-2} s^{-1} at 1 keV, $kT = 45^{+10}_{-8}$ eV and a blackbody radius of $R = 6.3^{+7.8}_{-3.4}$ km. The corresponding goodness-of-fit is $\chi^2 = 101.8$ for 86 d.o.f. which is statistically acceptable. The best-fit model and the observed spectra are shown in Figure 3.

We have also considered the spectral fit with a dual blackbody model. However, the goodness-of-fit yielded ($\chi^2 = 109.3$ for 85 d.o.f.) by this model is worse than the power-law plus blackbody model. Fixing the $n_{\rm H}$ at the Galactic HI value does not result in any improvement of the fitting.

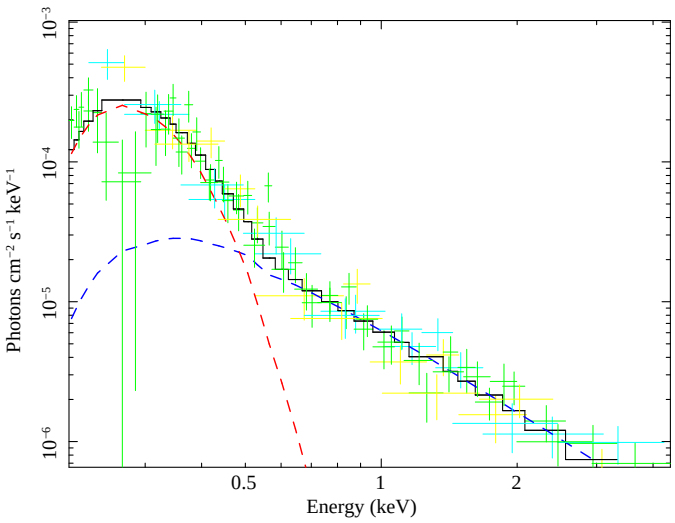

Fig. 3.— The phase-averaged X-ray spectra of PSR J1836+5925 as observed by *XMM-Newton* (MOS 1:cyan; MOS 2:yellow; PN:green) and simultaneously fitted to an absorbed power-law plus blackbody model. The best-fit model for the thermal (red-dashed line) and non-thermal (blue-dashed line) components are illustrated separately.

3. Discussion

In this Letter, we report the discovery of X-ray pulsations from PSR J1836+5925. We found that the pulsed events both contribute in soft and medium bands (0.2–2 keV). On the other hand, no indication of pulsation in the hard band (>2 keV) has been found in our investigation. The X-ray and γ-ray pulsation from PSR J1836+5925 have significantly different behavior. The pulsed γ-rays have a structure of relatively sharp double peaks which are presumably originated from the curvature radiation emitted from the pair creation region in the magnetosphere. The spin period of $P = 173$ ms and the characteristic age of $\tau = 1.8$ Myr suggest PSR J1836+5925 as a mature pulsar. Assumming the emission is isotropic, the GeV gamma-ray efficiency of PSR J1836+5925 is $\eta = (L_\gamma/\dot{E}) \times 100\% = 180 \pm 1^{+200}_{-100}\%$ (second *Fermi* pulsar catalog; Abdo et al. 2013), where $\dot{E}$ is the spin down power. The first uncertainty of η comes from the statistical uncertainties in the spectral fit and the second is due to the distance uncertainty (Abdo et al. 2013). This high efficiency of the GeV emission is similar to

$\eta = 97.4 \pm 0.3^{+300}_{-50}\%$ of typical mature pulsar — Geminga, if one assumes a 4π solid angle. Considering the possible overestimated distances and/or the beaming factor, the aforementioned conversion efficiencies can be overestimated. Taking the more realistic parameters into account, this might result in an efficiency $\eta < 100\%$.

In order to compare with Geminga, therefore, we discuss the origin of the X-ray emission of PSR J1836+5925. In the soft band (see Fig 2), the light curve is essentially sinusoidal which suggests the X-ray pulsation is mostly originated from the modulation of the heated polar cap. This is consistent with the presence of a blackbody component inferred from the spectral fit.

To account for the power-law component, we discuss it in the context of the outergap model (Cheng & Zhang 1998). According to this model, the non-thermal component of a canonical pulsar is synchrotron emission from the relativistic e^-/e^+ in the outer magnetospheric gap (Takata et al. 2006, 2008) with a week absorption. The photon index is expected to be in the range of 1.5–2.0 which is consistent with the best-fit value. For the light curve in 0.7-2 keV, its profile is apparently different from that in 0.2-0.7 keV which might suggests a different origin. In examining the relative flux contributions by the thermal and non-thermal component, we found that while the non-thermal flux takes $\sim 15\%$ in 0.2-0.7 keV its contribution is $> 99\%$ in 0.7-2 keV (see also Fig. 3). This suggests that X-ray pulsations seen in 0.2-0.7 keV and 0.7-2 keV might have different origin. However, the small photon statistics in the medium band precludes any firm conclusion. To better characterize the X-rays from PSR J1836+5925 in different energy bands, a deeper observation is certainly required. With a larger number of photons detected, we can also perform a phase-resolved spectroscopy to investigate how do the spectral properties vary across the rotational phase which will provide important inputs for a physical modeling of the pulsar.

We thank Mr. Jason H. K. Wu of Max-Planck-Institut *für* Radioastronomie for providing useful comments on the temporal analysis techniques. This work made use of data supplied by the High Energy Astrophysics Science Archive Research Center (HEASARC). This project is partially supported by the Ministry of Science and Technology of Taiwan through grant NSC 101-2112-M-039-001-MY3. C. Y .H. is supported by the research fund of Chungnam National University in 2014. J. T. is supported by a GRF grant of Hong-Kong Government under HKU700911P. C. P. H. and Y. C. are supported by the Ministry of Science and Technology of Taiwan through the grant NSC 102-2112-M-008-020-MY3. A. K. H. K. is supported by the Ministry of Science and Technology of Taiwan through grants NSC 100-2628-M-007-002-MY3 and NSC 100-2923-M-007-001-MY3. D. C. C. Y. gets the financial support from the Ministry of Science and Technology of Taiwan through the grant NSC 102-2115-M-030-003 and the other FJU project of A0502004.

REFERENCES

Abdo, A. A., et al. 2009, Science, 325, 840

—. 2010, ApJ, 712, 1209

—. 2013, ApJS, 208, 17

Bertsch, D. L., et al. 1992, Nature, 357, 306

Caraveo, P. A., De Luca, A., Marelli, M., Bignami, G. F., Ray, P. S., Saz Parkinson, P. M., & Kanbach, G. 2010, ApJ, 725, L6

Caraveo, P. A., De Luca, A., Mereghetti, S., Pellizzoni, A., & Bignami, G. F. 2004, Science, 305, 376

Cheng, K. S., & Zhang, L. 1998, ApJ, 498, 327

Edwards, R. T., Hobbs, G. B., & Manchester, R. N. 2006, MNRAS, 372, 1549

Halpern, J. P., Camilo, F., & Gotthelf, E. V. 2007, ApJ, 668, 1154

Halpern, J. P., Gotthelf, E. V., Mirabal, N., & Camilo, F. 2002, ApJ, 573, L41

Halpern, J. P., & Holt, S. S. 1992, Nature, 357, 222

Hobbs, G. B., Edwards, R. T., & Manchester, R. N. 2006, MNRAS, 369, 655

Kalberla, P. M. W., Burton, W. B., Hartmann, D., Arnal, E. M., Bajaja, E., Morras, R., & Pöppel, W. G. L. 2005, A&A, 440, 775

Kerr, M. 2011, ApJ, 732, 38

Leahy, D. A. 1987, A&A, 180, 275

Lin, L. C. C., Huang, R. H. H., Takata, J., Hwang, C. Y., Kong, A. K. H., & Hui, C. Y. 2010, ApJ, 725, L1

Lin, L. C. C., et al. 2013, ApJ, 770, L9

Marelli, M., et al. 2014, ArXiv e-prints

Mirabal, N., & Halpern, J. P. 2001, ApJ, 547, L137

Mirabal, N., Halpern, J. P., Eracleous, M., & Becker, R. H. 2000, ApJ, 541, 180

Takata, J., Chang, H., & Shibata, S. 2008, MNRAS, 386, 748

Takata, J., Shibata, S., Hirotani, K., & Chang, H.-K. 2006, MNRAS, 366, 1310

Trepl, L. et al. 2010, MNRAS, 405, 1339

Zhang, L., & Cheng, K. S. 1997, ApJ, 487, 370

This 2-column preprint was prepared with the AAS LaTeX macros v5.2.